This is a repository copy of *Energetic output of the 2022 Hunga Tonga–Hunga Ha'apai volcanic eruption from pressure measurements*.

White Rose Research Online URL for this paper:
https://eprints.whiterose.ac.uk/191410/

Version: Published Version

TECHNICAL NOTE

Energetic output of the 2022 Hunga Tonga–Hunga Ha'apai volcanic eruption from pressure measurements

J. S. Díaz[1] · **S. E. Rigby[2]**

Abstract

The violent eruption of the volcano at Hunga Tonga–Hunga Ha'apai island on January 15, 2022, generated an intense pressure wave registered by instruments all over the world. Using public reports posted on social media, we have used the arrival time of the first passage of the wave to measure its velocity, found to be a constant 1114 ± 2 km/h (309 ± 1 m/s). An empirical pressure–distance relation that utilizes measurements from a large range of sources is used to estimate an energetic output. We find that this Hunga Tonga–Hunga Ha'apai volcanic eruption released approximately the equivalent of 61 Mt, which is considerably larger than the 1980 eruption of Mount St. Helens and slightly higher than the yield of Tsar Bomba, the largest human-made explosion in history.

Keywords Volcanic explosion · Hunga Tonga–Hunga Ha'apai eruption · energetic output · Lamb wave

1 Introduction

The volcano at Hunga Tonga–Hunga Ha'apai island in the Kingdom of Tonga erupted in late 2021 and at the beginning of 2022 [1]. A violent eruption at 04:15 UTC on January 15, 2022 [2], produced a series of large explosions that generated pressure disturbances in Earth's atmosphere recorded by instruments worldwide at ground level and visible to many weather satellites in orbit [3]. Acoustic-gravity waves correspond to general solutions for the wave motion of the atmosphere as a compressible fluid under the presence of gravity. After some justified assumptions, different propagation modes of these acoustic-gravity waves can be identified. The long-amplitude mode that propagates parallel to the Earth's surface with a speed approximately 310 m/s maintained by hydrostatic equilibrium is known as a Lamb wave [4–8]. Weather stations registered a sudden

Communicated by E. Timofeev.

✉ S. E. Rigby
  sam.rigby@sheffield.ac.uk

  J. S. Díaz
  jsdiazpo@iu.edu

1 Physics Department, Indiana University, Bloomington, IN 47405, USA

2 Department of Civil and Structural Engineering, University of Sheffield, Mappin Street, Sheffield, S1 3JD, UK

increase in pressure rapidly followed by a negative phase before returning to ambient conditions. The pressure signals lasted approximately 45 min. Figure 1 shows the distinctive signature of the main pressure pulse observed as the waves passed moving toward the antipodal point in southern Algeria, reached later in the day around 22:30 UTC. As the news of the pressure wave traveling the globe spread, a large number of government agencies, professional meteorologists, and weather enthusiasts began sharing screenshots of the readings from their recording devices showing the Lamb-wave pulse on social media. Most of these images include time and pressure scales that, in addition to location information, allow establishing the time of arrival and evolution of the Lamb wave as it moved across the surface of the planet, circling the Earth several times [9,10]. In the upper atmosphere, the corresponding ionospheric disturbance has been recently studied using satellite measurements [11,12]. In addition to the intense pressure wave, the Hunga Tonga–Hunga Ha'apai volcano eruption generated a tsunami that reached all coasts on the Pacific Ocean but also the Caribbean Sea [13–15].

After any large explosive event, a characterization of the energy released becomes of great interest, e.g., [16–19]. A common practice is the report of this energy in terms of tonnes of TNT equivalent. A preliminary estimate based on material removed and motion of the eruption plume put the energetic output in the range 4–18 Mt [20]. Despite the

common use of units from explosion physics, we warn the reader that this only serves as a characterization of the energetic output of this type of volcanic eruption because the mechanisms behind are distinct from those of blast waves.

In this article, we use 124 pressure measurements obtained from images posted online, free weather web applications, and professional weather stations to characterize the speed of the Lamb wave. Additionally, a subset of 86 measurements were used to estimate the energetic output of the main eruption from the decay of the pressure pulse amplitude with distance. The result is presented in megatons of TNT equivalent as a way to directly compare with historically known explosive tests and, more relevant for the geophysical community, other explosive eruptions of volcanoes through history. Nonetheless, we emphasize that the mechanism and evolution of the pressure disturbance produced by a volcanic eruption greatly differs from a blast wave. For this reason, the analysis in this article is not based on results from the blast-wave literature; in fact, it makes no assumptions on the underlying mechanism that produced the pressure waves but rather only makes use of observable features of the Lamb wave. The method for determining the energetic output of the eruption presented in Sect. 4 is generic, and it can be used for any pressure-wave recordings.

2 Data

Early reports of the strong pressure wave appeared on Twitter as footage of loud explosions in the neighboring islands of the Fiji archipelago, such as Lakeba island located 440 km from Hunga Tonga–Hunga Ha'apai island [21]. As the hours passed and the Lamb wave reached New Zealand and Australia, more reports were posted primarily by local weather services but also by private users who began sharing screenshots of their own measurements on Twitter. Promptly, a worldwide community of weather enthusiasts engaged in a spontaneous and fascinating citizen science project. Although pressure measurements of the second and third passes of the wave exist, we only use measurements of the first pass that allow a clear identification of the time of arrival and determination of the amplitude of the pressure signal. The clearest feature observed in all the stations worldwide is the maximum recorded pressure, which we have used for timing the Lamb wave. Sampling rates varied from station to station. In most cases, data were recorded every few minutes, which was typically less than the rise time of the pulse, allowing for accurate determination of the arrival time and peak amplitude of the pressure pulse (see Fig. 1).

After collecting almost 100 such posts, we selected those that allowed a clear determination of local time and the location of the measurement. Local times were converted into UTC. The data set was extended by including
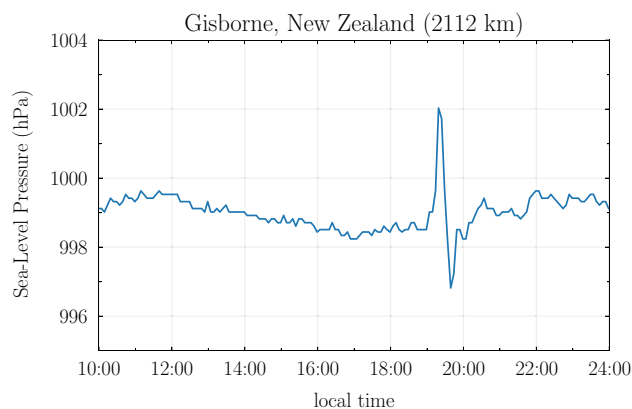

Fig. 1 Pressure data showing the pressure pulse registered in Gisborne, New Zealand, almost two hours after the main eruption

measurements from 40 weather stations accessible via the Historical Weather tool publicly provided by Weather Underground [22]. Of particular interest was any measurement in the nearby region of Hunga Tonga–Hunga Ha'apai island. One remarkable video posted on YouTube shows the multi-camera footage recorded from a distance of 73 km in Tongatapu, Tonga's main island, including detailed readings from two barometers during the arrival of the pressure wave [23]. The user kindly responded to our request to provide timing information in an extended version of the footage including time stamps, which gave us a valuable sample corresponding to the closest possible measurement to the erupting volcano [24]. On the opposite side of the planet, samples close to the antipodal point were obtained via the Balearic Islands Coastal Ocean Observing and Forecasting System [25] and the IRIS DMC Web Service [26]. Finally, we completed the full 124-sample data set after including measurements from 19 meteorological stations spread around the Fiji archipelago located between 350 and 900 km from Hunga Tonga–Hunga Ha'apai island. These samples were kindly provided by the Fiji Meteorological Service [27]. For each sample, the distance from the measurement location to Hunga Tonga–Hunga Ha'apai island was determined using `proj`, a Python interface for cartographic projections [28]. Figure 2 shows the worldwide distribution of measurement locations in the final data set.

For about 70% of the data set, a pressure scale was visible, which led to 86 measurements of the pressure amplitude relevant for the analysis presented in Sect. 4.
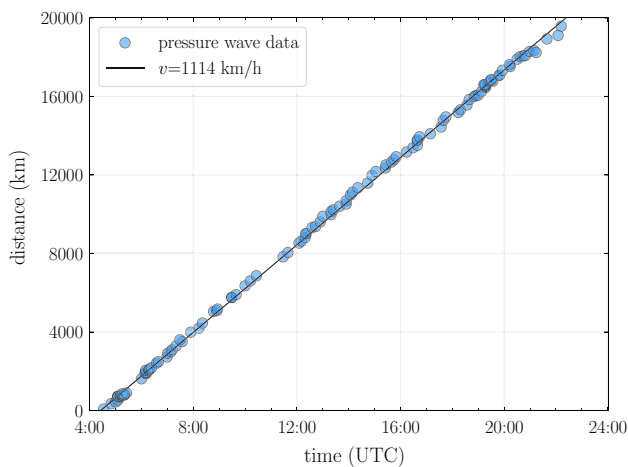
3 Speed of the Lamb wave

The data set described in Sect. 2 allows the determination of the speed of the pressure as it moved across the planet. Figure 3 shows the arrival time data of the Lamb wave at different locations, which follow a straight line, i.e., constant
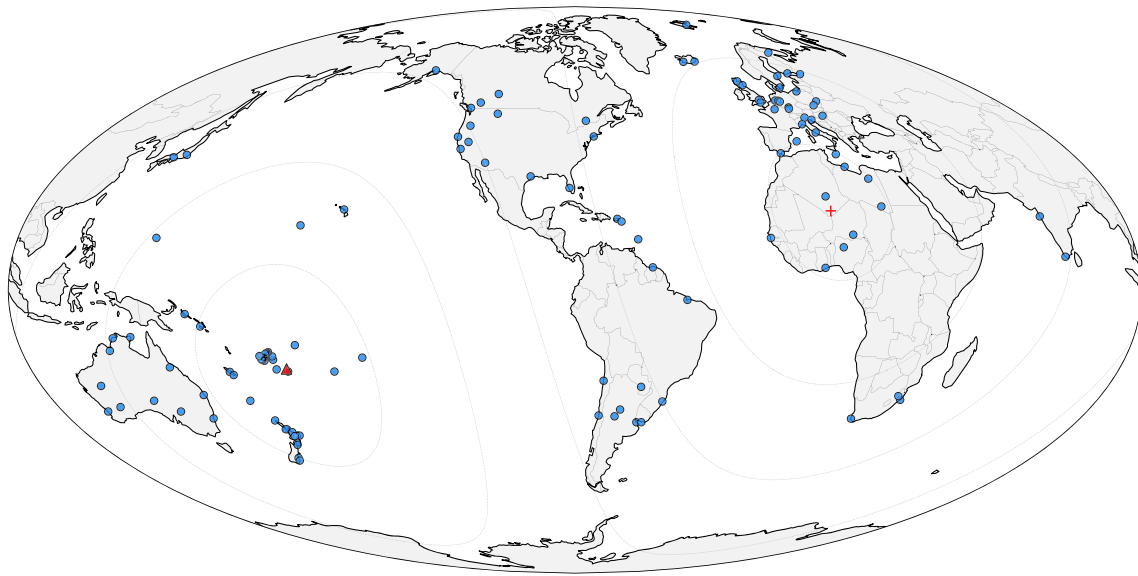
Fig. 2 Worldwide distribution of the 124 measurement locations in the final data set indicated by circles. The location of Hunga Tonga–Hunga Ha'apai island is denoted by the triangle, and the + marker indicates the antipodal point in southern Algeria. Distance at steps of 3000 km from the volcano is represented by the dashed lines

Fig. 3 Arrival of the Lamb wave at different locations over the planet. The data are properly described by a uniform motion at 1114 ± 2 km/h (309 ± 1 m/s)

velocity. The fit parameters to the data indicate the speed of the wave to be 1114 ± 2 km/h (309 ± 1 m/s), and the fitted intercept at $R_0 = -4927 \pm 33$ km implies that the main explosion occurred at approximately 04:25 UTC, several minutes after the first seismic event [2]. The speed determined here confirms that the pressure disturbance corresponds to a Lamb wave [4–6,8,29].

The speed determined here is in excellent agreement with speed of the pressure wave produced by the Krakatoa eruption in 1883, that during the first passage from the source had a constant value 1148 ± 10 km/h (319 ± 3 m/s) [30–32]. Similarly, our result agreed with the speed of the Lamb wave generated by the eruption of Mount St. Helens [33]. We emphasize that we have not attempted to separate measurements by their direction of propagation nor analyzed the individual path from the source to the measurement point; therefore, the speed determined above corresponds to an average value.

4 Decay of the pressure signal

The data set described in Sect. 2 can be used to study the decay of the pressure pulse over a long range of distances, which can be used to estimate the energetic output. Following studies of large-scale pressure waves produced by natural and artificial explosions, we define the pressure amplitude ΔP as the pressure difference between the maximum and the minimum of the pressure signal, also known as peak-to-trough amplitude [34–36]. Figure 4 shows the decay of pressure amplitude with propagation distance. An interesting feature appears with the most distant measurements from Hunga Tonga–Hunga Ha'apai island, as a noticeable increase in the pressure amplitude is observed. Since this pressure increase is a result of the coalescence of the Lamb wave at the antipodal point rather than any mechanism driven by the initial energetic output, samples from stations above 16,500 km (shown as open circles in Fig. 4) are excluded from the analysis below.

Independent of the physics underlying the generation of the observed Lamb wave, we simply attempt to determine the energetic output, E_0, using an empirical formulation. Since
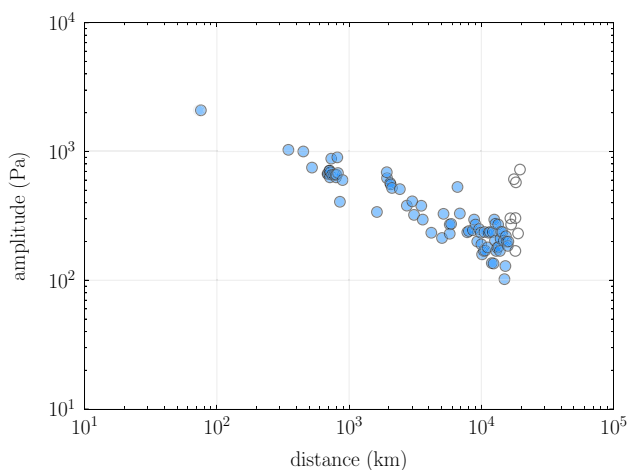
Fig. 4 Pressure amplitude measured at different distances from Hunga Tonga–Hunga Ha'apai island. The most distant measurements (open circles) exhibit a conspicuous increase in pressure as the wave approached the antipodal point

the amplitude of the pressure disturbance decreases as the wave propagates, we can write the amplitude of the pressure signal as a power law

$$\Delta P = A E_0^{\beta} R^{-\alpha}, \tag{1}$$

where the constants α, β, and A must be determined by calibration using some known energetic output producing a corresponding pressure disturbance measured at different distances R over the globe.

In order to calibrate the expression for the pressure amplitude and determining the free parameters in (1), we make use of two well-studied explosions that have triggered large-scale pressure waves measured worldwide. As for an explosive volcanic eruption, we consider the 1980 eruption of Mount St. Helens. With an estimated energy output of 7–35 Mt [37–41], the corresponding Lamb wave was measured by many surrounding stations starting at less than 100 km all the way

to over 8000 km with measurements in Japan and Europe [35,40,41]. The largest human-made explosion leading to a pressure wave observed over long distances is the thermonuclear test popularly known as the Tsar Bomba, detonated on October 30, 1961, by the Soviet Union at Severny Island with a yield of 58 Mt [42]. The signature of the pressure wave was registered by stations in Africa, Europe, and the USA [36,41,43–46], in addition to a rich collection of measurements in New Zealand [47]. The data from these two pressure waves are presented in Fig. 5, alongside our Hunga Tonga–Hunga Ha'apai data. Independent of any modeling, the data from Mount St. Helens show a distinctly shorter amplitude for the same distance than the Hunga Tonga–Hunga Ha'apai data, suggesting that the pressure wave from the recent eruption was generated by a much higher release of energy.

5 Results

Given the noise level that the data sets exhibit, a robust regression method is used instead of a standard squared error loss. The application of a Huber loss [48] limits the effects of potential outliers that could skew the fitting procedure.

Fitting the parameters α, β, and A to the Tsar Bomba and Mount St. Helens pressure data results in a stable value for the decay parameter $\alpha = 0.684$. The other two parameters exhibit a competing behavior, and their precise values are sensitive to the choice of energetic output for Mount St. Helens E_0^{SH}. The variation of all fit parameters as a function of E_0^{SH} is presented in Fig. 6. The horizontal line on the top panel confirms the stability of the decay parameter α. The second panel shows that that energy exponent β grows with E_0^{SH}, forcing the scale factor A to rapidly drop by several orders of magnitude. This variation in A drastically modifies the scale of the pressure amplitude. In the lower limit $E_0^{\text{SH}} = 7$ Mt, we find $\beta = 0.923$ and $A = 1395$, whereas in the upper limit $E_0^{\text{SH}} = 35$ Mt, we find $\beta = 3.863$ and

Fig. 5 Pressure amplitude measured at different distances from pressure waves produced by the 2022 eruption at Hunga Tonga–Hunga Ha'apai island, the Tsar Bomba, and the 1980 eruption of Mount St. Helens. Illustrative lines at different orders of magnitude for the energetic output are shown for the fit parameters resulting from choosing the lower bound for the energetic output of Mount St. Helens discussed in Sect. 5
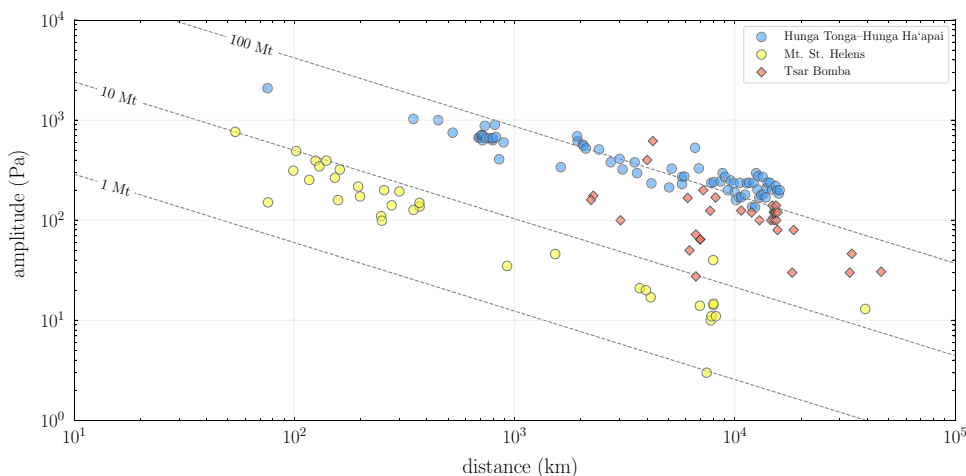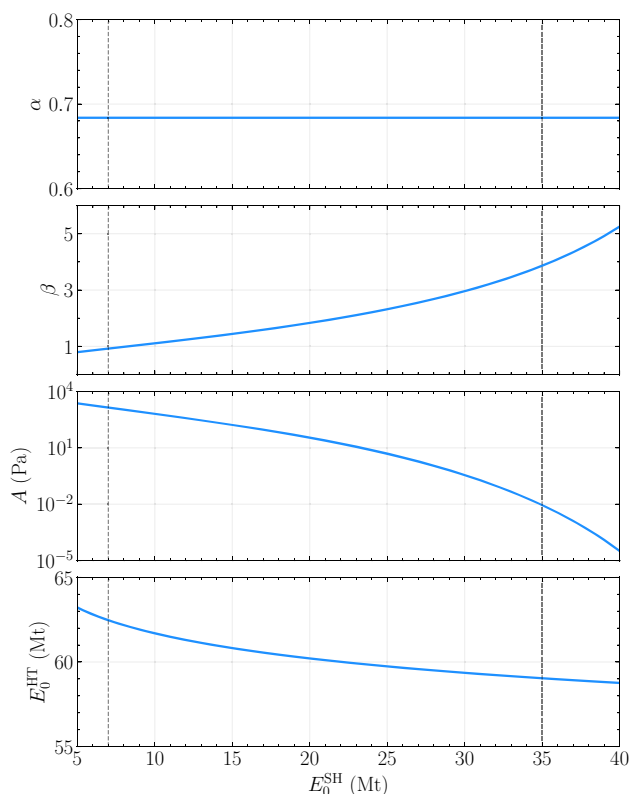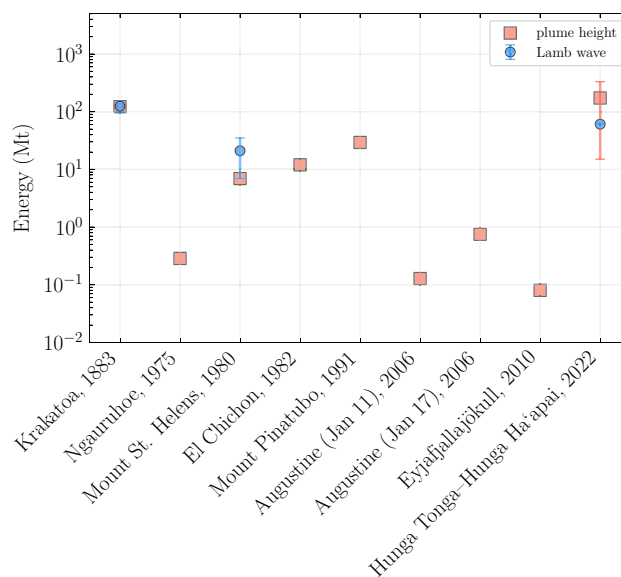
Fig. 6 Variation of the fitting parameters as a function of the choice of energetic output for Mount St. Helens E_0^{SH}, whose range is indicated by the vertical dashed lines. The decay parameter is constant (top panel), whereas the energy exponent β and the scale factor A compensate each other (middle panels). Despite this variability, the fit to the Hunga Tonga–Hunga Ha'apai data is stable leading to the energetic output $E_0^{\mathrm{HT}} = 59$–62 Mt

Fig. 7 Energetic output of explosive eruptions estimated from plume height and Lamb-wave measurements. Visible error bars indicate the accepted range of values for Mount St. Helens and uncertainty in the height for Hunga Tonga–Hunga Ha'apai

$A = 0.091$. Consequently, we fit the energy to the Hunga Tonga–Hunga Ha'apai data and found that the parameter E_0^{HT} is stable to the choice of E_0^{SH}. In other words, despite the wide variations of β and A, the fit of the energy to the Hunga Tonga–Hunga Ha'apai data remains within the range 59–62 Mt. For comparison, the violent eruption of Krakatoa volcano in 1883 is estimated to have released an energetic output in the range 100–150 Mt [32,49].

This result suggests that the violent eruption of Hunga Tonga–Hunga Ha'apai volcano generated a Lamb wave similar to that produced by the detonation of the Tsar Bomba. Lines at different orders of magnitude for the energetic output are included in Fig. 5 for comparison.

6 Comparison with other explosive eruptions

The eruption of Krakatoa in 1883 or Mount St. Helens in 1980 are representative examples of explosive eruptions producing a Lamb wave of global scale. In Fig. 7, we present

the energetic output from these two eruptions obtained from Lamb-wave measurements. The range for Krakatoa was obtained by Harkrider and Press using scaling methods to match the pressure pulse observed compared to those from nuclear tests [32]. Several authors have applied a similar approach to the data from Mount St. Helens [37–41]; the accepted range for the energetic output is represented by the error bar. Finally, we also include the result from Sect. 5 for Hunga Tonga–Hunga Ha'apai. Morton et al. found that for explosive eruptions the energetic output (in joules) can be determined from the height H (in meters) of the buoyant volcanic plume using the relation $Q = (H/1.87)^4$ [50]. Detailed monitoring of volcanoes such as Mt. Ngāuruhoe [51,52], Augustine [53], and Eyjafjallajökull [54] can be used to estimate the energetic output by some of their explosive eruptions from measurements of their plume height. Using the energy–height relation, we have estimated the energetic outputs in some eruptions of the mentioned volcanoes and include them in Fig. 7 for comparison. The height in kilometers used for each of the eruptions shown in Fig. 7 is, respectively: Krakatoa, 50.0 [31]; Ngāuruhoe, 11.0 [51,52]; Mount St. Helens, 24.4 [55]; El Chichón, 28.0 [56]; Mount Pinatubo, 35.0 [57]; Augustine (Jan 11), 9.0; Augustine (Jan 17), 14.0 [53]; and Eyjafjallajökull, 8.0 [54]. There still is some uncertainty in the height of the plume generated by the eruption at Hunga Tonga–Hunga Ha'apai, the error bar in Fig. 7 represents this uncertainty for the energy obtained in the range 30.0–60.0 km [1,58]. The figure shows that the estimate from the Lamb-wave amplitude decay found in Sect. 5 is consistent with the plume estimate. It can be seen

that the Hunga Tonga–Hunga Haʻapai eruption ranks as one of the most energetic volcanic eruptions in recent history.

7 Closing remarks

A data set characterizing the amplitude of the Lamb wave generated by the eruption of Hunga Tonga–Hunga Haʻapai volcano on January 15, 2022, was constructed from social media posts. Additionally, the data set was highly enriched by including publicly available data from worldwide professional stations. Timing measurements and distance information were used to determine that the Lamb wave moved from the source at a constant speed of 1114 ± 2 km/h (309 ± 1 m/s), similar to the observed speed of these type of waves from eruptions in the past and consistent with the expected speed of an atmospheric Lamb wave [4–6,8]. We employed an empirical description of the decay of the amplitude of the pressure wave as a function of distance and fit the free parameters to data from pressure waves produced by volcanic eruptions and thermonuclear tests. Subsequently, we applied the empirical relation to the Hunga Tonga–Hunga Haʻapai data and determined that the corresponding Lamb wave was generated by the energetic output of approximately 61 Mt. This estimate is about five times that of preliminary reports, and it suggests that the eruption at Hunga Tonga–Hunga Haʻapai producing the vast pressure wave that circled the Earth several times in January 2022 was slightly higher in magnitude than the yield of the Tsar Bomba in 1961. Our result is in excellent agreement with preliminary estimates from teleseismic [59], infrasound [60], and seismoacoustic measurements [61].

In early 1884, members of the *Krakatoa Committee* organized by the Royal Society resolved to publish in *The Times* and other publications an invitation to the public to share any observations that could have scientific value, from dust and pumice observed in the shores to barometric measurements, locations where the explosion was heard, and other atmospheric phenomena [31,62]. In a similar fashion, after the eruption of Mount St. Helens in 1980, the president of the European Seismological Commission reported on their request to meteorological services all over the world to share pressure data to study the wave propagation [63]. In this article, we have used information publicly shared from all regions of the world to create a data set within days of the eruption at Hunga Tonga–Hunga Haʻapai island, demonstrating that social media can serve as a valuable source of data connecting citizen scientists worldwide.

Declaration

References

1. Global Volcanism Program, 2022. Report on Hunga Tonga-Hunga Ha'apai (Tonga). In: Sennert, S. K. (ed.), Weekly Volcanic Activity Report, 12–18 January 2022, Smithsonian Institution and US Geological Survey (2022). https://doi.org/10.5479/si.GVP.WVAR20220112-243040https://volcano.si.edu/ShowReport.cfm?doi=10.5479/si.GVP.WVAR20220112-243040

2. USGS, M 5.8 Volcanic Eruption (2022). https://earthquake.usgs.gov/earthquakes/eventpage/pt22015050. Accessed 20 Jan 2022

3. Baines, P.G., Sacks, S.: The generation and propagation of atmospheric internal waves caused by volcanic eruptions. Atmosphere **8**(3), 60 (2017). https://doi.org/10.3390/atmos8030060

4. Lamb, H.: On the vibrations of an elastic sphere. Proc. Lond. Math. Soc. **1**, 189–212 (1881). https://doi.org/10.1112/plms/s1-13.1.189

5. Garrett, C.J.R.: Atmospheric edge waves. Q. J. R. Meteorol. Soc. **95**, 731–753 (1969). https://doi.org/10.1002/qj.49709540607

6. Pierce, A.D., Posey, J.W.: Theory of the excitation and propagation of Lamb's atmospheric edge mode from nuclear explosions. Geophys. J. Int. **26**, 341–368 (1971). https://doi.org/10.1111/j.1365-246X.1971.tb03406.x

7. Lindzen, R.S., Blake, D.: Lamb waves in the presence of realistic distributions of temperature and dissipation. J. Geophys. Res. **77**, 2166–2176 (1972). https://doi.org/10.1029/JC077i012p02166

8. Nishida, K., Kobayashi, N., Fukao, Y.: Background Lamb waves in the Earth's atmosphere. Geophys. J. Int. **196**, 312–316 (2014). https://doi.org/10.1093/gji/ggt413

9. Duncombe, J.: The surprising reach of Tonga's giant atmospheric waves. EOS Sci. News AGU (2022). https://doi.org/10.1029/2022EO220050

10. Amores, A., Monserrat, S., Marcos, M., Argüeso, D., Villalonga, J., Jordà, G., Gomi, D.: Numerical simulation of atmospheric Lamb waves generated by the 2022 Hunga–Tonga volcanic eruption. Geophys. Res. Lett. **49**(6), e2022GL098240 (2022). https://doi.org/10.1029/2022GL098240

11. Themes, D.R., Watson, C., Žagar, N., Vasylkevych, S., Elvidge, S., Mccaffrey, A., Prikryl, P., Reid, B., Wood, A., Jayachandran, P.T.: Global propagation of ionospheric disturbances associated with the 2022 Tonga Volcanic Eruption. Earth Space Sci. Open Arch. (2022). https://doi.org/10.1002/essoar.10510350.1

12. Zhang, S.R., Vierinen, J., Aa, E., Goncharenko, L., Erickson, P., Rideout, W., Coster, A., Andres Spicher, A.: 2022 Tonga volcanic eruption induced global propagation of ionospheric disturbances via Lamb waves. Earth Space Sci. Open Arch. (2022). https://doi.org/10.1002/essoar.10510445.1

13. Pacific Tsunami Warning Center: bulletin tsunami message number 1 (2022). https://tsunami.gov/events/PHEB/2022/01/15/22015050/1/WEZS40/WEZS40.txt. Accessed 20 Jan 2022

14. NOAA National Centers for Environmental Information: January 15, 2022 Tonga Tsunami (2022). https://www.ngdc.noaa.gov/hazard/dart/2022tonga.html. Accessed 20 Jan 2022

15. Ramírez-Herrera, M.T., Coca, O., Vargas-Espinosa, V.: Tsunami effects on the coast of Mexico by the Hunga Tonga–Hunga Ha'apai volcano eruption. Tonga. Pure Appl. Geophys. **179**(4), 1117–1137 (2022). https://doi.org/10.1007/s00024-022-03017-9

16. Rigby, S.E., Lodge, T.J., Alotaibi, S., Barr, A.D., Clarke, S.D., Langdon, G.S., Tyas, A.: Preliminary yield estimation of the 2020 Beirut explosion using video footage from social media. Shock Waves **30**, 671–675 (2020). https://doi.org/10.1007/s00193-020-00970-z

17. Díaz, J.S.: Explosion analysis from images: Trinity and Beirut. Eur. J. Phys. **42**, 035803 (2021). https://doi.org/10.1088/1361-6404/abe131

18. Pilger, C., Gaebler, P., Hupe, P., Kalia, A.C., Schneider, F.M., Steinberg, A., Sudhaus, H., Ceranna, L.: Yield estimation of the 2020 Beirut explosion using open access waveform and remote sensing data. Sci. Rep. **11**, 14144 (2021). https://doi.org/10.1038/s41598-021-93690-y

19. Aouad, C.J., Chemissany, W., Mazzali, P., Temsah, Y., Jahami, A.: Beirut explosion: TNT equivalence from the fireball evolution in the first 170 milliseconds. Shock Waves **31**, 813–827 (2021). https://doi.org/10.1007/s00193-021-01031-9

20. NASA Earth Observatory: dramatic changes at Hunga Tonga-Hunga Ha'apai (2022). https://earthobservatory.nasa.gov/images/149367/dramatic-changes-at-hunga-tonga-hunga-haapai. Accessed 08 Feb 2022

21. https://twitter.com/portiajessene/status/1482331548330659841 (2022). Accessed 16 Jan 2022

22. Historical Weather, Weather Underground. https://wunderground.com/history. Accessed 16 Jan 2022

23. Delmar, M.: Tonga volcanic eruption as seen from Tonga 73 kilometers away (2022). https://youtube.com/watch?v=vn1Gfqd6SK4. Accessed 02 Feb 2022

24. Delmar, M.: Extended footage-Tongas Jan15th volcanic eruption Hunga Tonga Hunga Ha'apai as seen from the ground (2022). https://www.youtube.com/watch?v=3US-AxvGfE4. Accessed 22 Feb 2022

25. Balearic Islands Coastal Ocean Observing and Forecasting System (2022). https://www.socib.es/. Accessed 23 Jan 2022

26. IRIS Data Service: NSF Incorporated Research Institutions for Seismology (2022). https://ds.iris.edu/ds/nodes/dmc/data. Accessed 23 Jan 2022

27. Historical Meteorological Data Request Form, Fiji Meteorological Service (2022). https://met.gov.fj/index.php?page=datarequest. Accessed 18 Jan 2022

28. Whitaker, J.: `proj` Python interface to PROJ v.3.3.0 (2021). https://pyproj4.github.io/pyproj

29. Vergoz, J., Hupe, P., Listowski, C., Le Pichon, A., Garcés, M.A., Marchetti, E., Labazuy, P., Ceranna, L., Pilger, C., Gaebler, P., Näsholm, S.P., Brissaud, Q., Poli, P., Shapiro, N., De Negri, R., Mialle, P.: IMS observations of infrasound and acoustic-gravity waves produced by the January 2022 volcanic eruption of Hunga, Tonga: a global analysis. Earth Planet. Sci. Lett. **591**, 117639 (2022). https://doi.org/10.1016/j.epsl.2022.117639

30. Taylor, G.I.: Waves and tides in the atmosphere. Proc. R. Soc. Lond. **A126**, 169–183 (1929). https://doi.org/10.1098/rspa.1929.0213

31. Symons, G.J.: The Eruption of Krakatoa and Subsequent Phenomena, Report of the Krakatoa Committee of the Royal Society. Trübner and Co., London (1888). https://doi.org/10.1002/qj.4970146809

32. Harkrider, D., Press, F.: The Krakatoa air-sea waves: an example of pulse propagation in coupled systems. Geophys. J. R. Astr. Soc. **13**, 149–159 (1967). https://doi.org/10.1111/j.1365-246X.1967.tb02150.x

33. Liu, C.H., Klostermeyer, J., Yeh, K.C., Jones, T.B., Robinson, T., Holt, O., Leitinger, R., Ogawa, T., Sinno, K., Kato, S., Ogawa, T., Bedard, A.J., Kersley, L.: Global dynamic responses of the atmosphere to the eruption of Mount St. Helens on May 18, 1980. J. Geophys. Res. Space Phys **87**(A8), 6281–6290 (1982). https://doi.org/10.1029/JA087iA08p06281

34. Pierce, A.D., Posey, J.W., Iliff, E.F.: Variation of nuclear explosion generated acoustic-gravity wave forms with burst height and with energy yield. J. Geophys. Res. **76**(21), 5025–5042 (1971). https://doi.org/10.1029/JC076i021p05025

35. Banister, J.R.: Pressure wave generated by the Mount St. Helens eruption. J. Geophys. Res. **89**(D3), 4895–4904 (1984). https://doi.org/10.1029/JD089iD03p04895

36. McKisic, J.M.: Infrasound and the infrasonic monitoring of atmospheric nuclear explosions: a literature review. OSTI Report AD-A-339249/5/XAB (1997). https://www.osti.gov/biblio/621445-infrasound-infrasonic-monitoring-atmospheric-nuclear-explosions-literature-review-final-report-september-february Report AD-A-339249/5/XAB

37. Kieffer, S.: Blast dynamics at Mount St. Helens on 18 May 1980. Nature **291**, 568–570 (1981). https://doi.org/10.1038/291568a0

38. Ritsema, A.R.: Observations of Mount St. Helens eruption. EOS Trans. AGU **61**(49), 1202–1202 (1980). https://doi.org/10.1029/EO061i049p01202-01

39. Bolt, B.A., Tanimoto, T.: Atmospheric oscillations after the May 18, 1980 eruption of Mount St. Helens. EOS Trans. AGU **62**(23), 529–530 (1981). https://doi.org/10.1029/EO062i023p00529

40. Donn, W.L., Balachandran, N.K.: Mount St. Helens eruption of 18 May 1980: air waves and explosive yield. Science **213**(4507), 539–541 (1981). https://doi.org/10.1126/science.213.4507.539

41. Reed, J.W.: Air pressure waves from Mount St. Helens eruptions. J. Geophys. Res. **92**(D10), 11979–11992 (1987). https://doi.org/10.1029/JD092iD10p11979

42. Sublette, C.: Big Ivan, The Tsar Bomba. Nuclear weapon archive (2007). http://nuclearweaponarchive.org/Russia/TsarBomba. Accessed 20 Jan 2022

43. Wexler, H., Hass, W.A.: Global atmospheric pressure effects of the October 30, 1961, explosion. J. Geophys. Res. **67**, 3875–3887 (1962). https://doi.org/10.1029/JZ067i010p03875

44. Araskog, R., Ericsson, U., Wägner, H.: Long-range transmission of atmospheric disturbances. Nature **193**, 970–971 (1962). https://doi.org/10.1038/193970a0

45. Jones, R.V.: Sub-acoustic waves from large explosions. Nature **193**, 229–232 (1962). https://doi.org/10.1038/193229a0

46. Donn, W.L., Shaw, D.M., Hubbard, A.C.: The microbarograph detection of nuclear explosions. IEEE Trans. Nucl. Sci. **10**, 285–296 (1963). https://doi.org/10.1109/TNS.1963.4323271

47. Farkas, E.: Transit of pressure waves through New Zealand from the Soviet 50 megaton bomb explosion. Nature **4817**, 765–766 (1962). https://doi.org/10.1038/193765a0

48. Huber, P.J.: Robust estimation of a location parameter. Ann. Math. Stat. **35**(1), 73–101 (1964). https://doi.org/10.1214/aoms/1177703732

49. Yokoyama, I.: A geophysical interpretation of the 1883 Krakatau eruption. J. Volcanol. Geotherm. Res. **9**, 359–378 (1981). https://doi.org/10.1016/0377-0273(81)90044-5

50. Morton, B.R., Taylor, G.I., Turner, J.S.: Turbulent gravitational convection from maintained and instantaneous sources. Proc. R. Soc. Lond. **A234**, 1–23 (1956). https://doi.org/10.1098/rspa.1956.0011

51. Nairn, I.A.: Atmospheric shock waves and condensation clouds from Ngauruhoe explosive eruptions. Nature **259**, 190–192 (1976). https://doi.org/10.1038/259190a0

52. Nairn, I.A., Self, S.: Explosive eruptions and pyroclastic avalanches from Ngauruhoe in February 1975. J. Volcanol. Geotherm. Res. **3**(1), 39–60 (1978). https://doi.org/10.1016/0377-0273(78)90003-3

53. Caplan-Auerbach, J., Bellesiles, A., Fernandes, J.K.: Estimates of eruption velocity and plume height from infrasonic recordings of the 2006 eruption of Augustine volcano. Alaska. J. Volcanol. Geotherm. Res. **189**(1), 12–18 (2010). https://doi.org/10.1016/j.jvolgeores.2009.10.002

54. Ripepe, M., Bonadonna, C., Folch, A., Delle Donne, D., Lacanna, G., Marchetti, E., Höskuldsson, A.: Ash-plume dynamics and eruption source parameters by infrasound and thermal imagery: the 2010 Eyjafjallajökull eruption. Earth Planet. Sci. Lett. **366**, 112–121 (2013). https://doi.org/10.1016/j.epsl.2013.02.005

55. Brantley S., Myers, B.: Mount St. Helens—from the 1980 eruption to 2000. U.S. Geological Survey Fact Sheet, 036-00. https://pubs.usgs.gov/fs/2000/fs036-00 (2005). Accessed 31 Jan 2022

56. Tilling, R.I.: El Chichón's surprise eruption in 1982: lessons for reducing volcano risk. Geofis. Int. **48**(1), 3–19 (2009). (https://pubs.er.usgs.gov/publication/70035886)

57. Newhall, C, Hendley, J.W., Stauffer, P.H.: The cataclysmic 1991 eruption of Mount Pinatubo, Philippines. U.S. Geological Survey Fact Sheet, pp. 113-197 (2005). https://pubs.usgs.gov/fs/1997/fs113-97/. Accessed 16 Feb 2022

58. NASA Earth Observatory: Tonga volcano plume reached the mesosphere (2022). https://earthobservatory.nasa.gov/images/149474/. Accessed 08 Feb 2022

59. Poli, P., Shapiro, N.: Rapid characterization of large volcanic eruptions: measuring the impulse of the Hunga Tonga Ha'apai explosion from teleseismic waves. Geophys. Res. Lett. **49**(8), e2022GL098123 (2022). https://doi.org/10.1029/2022GL098123

60. Kulichkov, S.N., Chunchuzov, I.P., Popov, O.E., Gorchakov, G.I., Mishenin, A.A., Perepelkin, V.G., Bush, G.A., Skorokhod, A.I., Vinogradov, Yu.A., Semutnikova, E.G., Sepic, J., Medvedev, I.P., Gushchin, R.A., Kopeikin, V.M., Belikov, I.B., Gubanova, D.P., Karpov, A.V., Tikhonov, A.V.: Rapid characterization of large volcanic eruptions: measuring the impulse of the Hunga Tonga Ha'apai explosion from teleseismic waves. Earth Planet. Sci. Lett. **591**, 117639 (2022). https://doi.org/10.1016/j.epsl.2022.117639

61. Matoza, R.S., Fee, D., Assink, J.D., Iezzi, A.M., Green, D.N., Kim, K., Toney, L., Lecocq, T., Krishnamoorthy, S., Lalande, J., Nishida, K., Gee, K.L., Haney, M.M., Ortiz, H.D., Brissaud, Q., Martire, L., Rolland, L., Vergados, P., Nippress, A., Park, J., Shani-Kadmiel, S., Witsil, A., Arrowsmith, S., Caudron, C., Watada, S., Perttu, A.B., Taisne, B., Mialle, P., Pichon, A.L., Vergoz, J., Hupe, P., Blom, P.S., Waxler, R., Angelis, S.D., Snively, J.B., Ringler, A.T., Anthony, R.E., Jolly, A.D., Kilgour, G., Averbuch, G., Ripepe, M., Ichihara, M., Arciniega-Ceballos, A., Astafyeva, E., Ceranna, L., Cevuard, S., Che, I., Negri, R.D., Ebeling, C.W., Evers, L.G., Franco-Marin, L.E., Gabrielson, T.B., Hafner, K., Harrison, R.G., Komjathy, A., Lacanna, G., Lyons, J., Macpherson, K.A., Marchetti, E., McKee, K.F., Mellors, R.J., Mendo-Pérez, G., Mikesell, T.D., Munaibari, E., Oyola-Merced, M., Park, I., Pilger, C., Ramos, C., Ruiz, M.C., Sabatini, R., Schwaiger, H.F., Tailpied, D., Talmadge, C., Vidot, J., Webster, J., Wilson, D.C.: Atmospheric waves and global seismoacoustic observations of the: Hunga eruption. Science, Tonga (2022). https://doi.org/10.1126/science.abo7063

62. Morgan, M.R.: The eruption of Krakatoa (also known as Krakatau) in 1883. BRANCH: Britain, Representation and Nineteenth-Century History (2013). https://branchcollective.org/?ps_articles=monique-morgan-the-eruption-of-krakatoa-also-known-as-krakatau-in-1883. Accessed 03 Feb 2022

63. Ritsema, A.R.: Atmospheric pressure wave of St. Helens eruption. Dev. Solid Earth Geophys. **15**, 311–317 (1983). https://doi.org/10.1016/B978-0-444-99662-6.50064-2

64. Kluyver, T., Ragan-Kelley, B., Pérez, F., Granger, B., Bussonnier, M., Frederic, J., Kelley, K., Hamrick, J., Grout, J., Corlay, S., Ivanov, P., Avila, D., Abdalla, S., Willing, C.: Jupyter Notebooks: a publishing format for reproducible computational workflows. In: Loizides F., Schmidt B. (eds) Positioning and Power in Academic Publishing: Players, Agents and Agendas, 87–90 (2016). https://doi.org/10.3233/978-1-61499-649-1-87

65. Array programming with NumPy: Harris, C.R., Millman, K.J., van der Walt, S.J., Gommers, R., Virtanen, P., Cournapeau, D., Wieser, E., Taylor, J., Berg, S., Smith, N.J., Kern, R., Picus, M., Hoyer, S., van Kerkwijk, M.H., Brett, M., Haldane, A., Fernández del Río, J., Wiebe, M., Peterson, P., Gérard-Marchant, P., Sheppard, K., Reddy, T., Weckesser, W., Abbasi, H., Gohlke, C., Oliphant, T.E. Nature **585**, 357–362 (2020). https://doi.org/10.1038/s41586-020-2649-2

66. Virtanen, P., Virtanen, P., Gommers, R., Oliphant, T.E., Haberland, M., Reddy, T., Cournapeau, D., Burovski, E., Peterson, P., Weckesser, W., Bright, J., van der Walt, S.J., Brett, M., Wilson, J., Millman, K.J., Mayorov, N., Nelson, A.R.J., Jones, E., Kern, R., Larson, E., Carey, C.J., Polat, I., Feng, Y., Moore, E.W., VanderPlas, J., Laxalde, D., Perktold, J., Cimrman, R., Henriksen, I., Quintero, E.A., Harris, C.R., Archibald, A.M., Ribeiro, A.H., Pedregosa, F., van Mulbregt, P., SciPy 1.0 Contributors: SciPy 1.0: fundamental algorithms for scientific computing in Python. Nature Methods **17**(3), 261–272 (2020). https://doi.org/10.1038/s41592-019-0686-2

67. McKinney, W.: Data structures for statistical computing in Python. In: Proceedings of the 9th Python in Science Conference, pp. 51–56 (2010). https://doi.org/10.25080/Majora-92bf1922-00a

68. Hunter, J.D.: Matplotlib: a 2D graphics environment. Comput. Sci. Eng. **9**, 90–95 (2007). https://doi.org/10.1109/MCSE.2007.55

69. UK Met Office: Cartopy, Python package for geospatial data processing, v.0.20.2 (2022). https://pypi.org/project/Cartopy

Publisher's Note Springer Nature remains neutral with regard to jurisdictional claims in published maps and institutional affiliations.